ELSEVIER

Physica C 337 (2000) 229–233

PHYSICA C

www.elsevier.nl/locate/physc

Critical current density in high-T_c Bi-2223 single crystals using AC and DC magnetic measurements

Shaoyan Chu, M.E. McHenry *

Department of Materials Science and Engineering, Carnegie Mellon University, Pittsburgh, PA 15213, USA

Abstract

Single crystals of $(Bi, Pb)_2Sr_2Ca_2Cu_3O_x$ ($T_c = 110$ K), prepared by fused-salt reaction technique [S.-Y. Chu, M.E. McHenry, J. Mater. Res. 13 (1998) 589; S.-Y. Chu, M.E. McHenry, IEEE Trans. Appl. Supercond. 7 (1997) 1150; S.-Y. Chu, M.E. McHenry, Electrochem. Soc. Proc. 97-2 (1997) 9.], have been characterized by both DC and AC magnetic measurements between 5 K and 108 K with a magnetic field perpendicular to the *ab* plane of the Bi-2223 crystal lattice. A numerical calculation indicates that the induced fields from the superconducting current loops in the separated neighboring crystals are very small and consequently can be neglected. Treating the individual crystals ($73 \times 73 \times 1$ μm^3) as bar-shaped superconductors, we used a modified Bean model to determine the critical current density. For the first time, a strong temperature dependence of the current density at zero applied field is observed in these pristine single crystals with weak pinning. These then offer an excellent model system to probe the enhancements of persistent currents by means of proton irradiation. © 2000 Published by Elsevier Science B.V.

1. Introduction

''Bulk'' applications of high-temperature superconductors (HTS) will require wires or tapes with high current densities J_c sustainable at high operating temperatures in magnetic field of several tesla. The knowledge of the J_c behavior as a function of temperature and magnetic field is therefore essential. An initial significant step towards a practical high-J_c superconductor was the development of the silver-sheathed, powder-in-tube tapes having the Bi-2223 phases as the majority component. It has been widely accepted that the formation of weak links at the grain boundaries and giant flux creep within grains having weak flux pinning potentials limit the J_c in the ceramic materials [1]. Interestingly, the intrinsic values of the critical current densities in single crystals with pure Bi-2223 phase have never been measured for lack of large enough homogenous samples. Detailed analysis of experimental data was performed to evaluate J_c in Bi-2223 grains in polycrystalline samples where both intergrain current and intragrain current contributed to the magnetic moment [2]. However, the problem dealing with mutual inductance due to other nearby grains may also be necessary to consider.

Recent achievement in growth of Bi-2223 single crystals ($T_c = 110$ K) provided us with high-quality specimen to carry out a contactless measurement of J_c [3]. As opposed to polycrystalline samples, our specimen is a collection of oriented single crystals

* Corresponding author. Fax: +1-412-268-3113.
E-mail address: sc79@andrew.cmu.edu (M.E. McHenry).

0921-4534/00/$ - see front matter © 2000 Published by Elsevier Science B.V.
PII: S0921-4534(00)00107-6

separated from each other with large enough space to avoid dipolar interactions. In this case, not only can the intergrain current effect be ruled out, but also the mutual inductance effect is very small. The present paper addresses the intrinsic persistent current density in the *ab* plane of the Bi-2223 phase. In Section 2, we will describe specimen details and the measurement technique that separates the mutual inductance effects. An analysis of the experimental data along with the modified Bean model and the behaviors of J_c of the pristine crystals in zero field are discussed in Section 3.

2. Specimen preparation and experimental details

$(Bi, Pb)_2Sr_2Ca_2Cu_3O_x$ single crystals were grown using a fused-salt reaction technique. The characterization of the magnetic properties of the high-quality crystals (with $T_c = 110$ K) has been described in detail [3,4]. The specimen used in this work consisted of a collection of 472 crystals pressed into a piece of indium foil with *c*-axes aligned normal to the foil. The average dimensions $2a \times 2b = 73$ μm $\times 73$ μm and the thickness $2d = 1$ μm (along the *c*-axis) of the crystals were determined by optical microscopy and SEM. A small amount ($< 3\%$) of Bi-2212 crystals, due to accidental selection, should not have an important effect on the magnetization measurement. A number of X-ray diffraction patterns for individual single crystals confirm the phase purity of Bi-2223 [5]. Both DC and AC magnetic moments of the specimen, measured at low field, indicate that the response from impurity superconducting phases is under the detectable limit.

A SQUID magnetometer (Quantum Design, MPMSR2) was used to measure DC magnetic moments of the specimen as a function of field at 20 different temperatures. The temperature dependence of the real and the imaginary part of the AC magnetic moment (i.e. $\boldsymbol{M}'$ and $\boldsymbol{M}''$) were measured for 10 different values of the drive AC magnetic field ($f = 83$ Hz) using a Quantum Design, PPMS AC susceptometer. The magnetic fields were always applied along the *c*-axis of the Bi-2223 crystals for both DC and AC magnetization measurements. It is worth mentioning that the origin of the measured magnetization of the present specimen is very different from that of a polycrystalline bulk or a mass of powder. For a polycrystalline sample, the detected magnetic moment, from which the J_c is inferred, is produced by contributions of both of intragrain current and intergrain currents. Moreover, for an individual grain, an external magnetic field implies not only the applied field supplied by a magnet (superconducting solenoid in a SQUID magnetometer, for instance), but also a local ''external'' magnetic field distribution contributed by a magnetic dipole of each individual grain even if the intergrain current can be neglected in some cases [2].

Superconducting current loops in an individual crystal give rise to magnetic dipole moments $\boldsymbol{m}_i$, at a point r_i. A local external magnetic induction at distant points r ($|r - r_i| \gg a \sim 36.5$ μm) can be expressed (in mks units):

$$\mathbf{B}_i \approx \frac{\mu_0}{4\pi} \frac{\mathbf{m}_i}{|r - r_i|^3} \tag{1}$$

where μ_0 is the permeability of free space. A total local external induced field distribution can be estimated to be:

$$\mathbf{B} \approx \frac{\mu_0}{4\pi} \sum_i \frac{\mathbf{m}_i}{|r - r_i|^3} \tag{2}$$

The direction of the total local external field $\boldsymbol{B}$ (or $\boldsymbol{H}$) depends on the magnetic dipole moment (due to shielding currents) being parallel to the applied field, i.e. *c*-axis of the Bi-2223 crystal lattice. The magnitude of the local external field in each crystal induced by all other crystals is:

$$\mathbf{H}' = \frac{\mu_0}{4\pi} \left(\frac{1}{471} \sum_i \frac{\mathbf{M}}{r_i^3} \right) \tag{3}$$

Here, $\boldsymbol{M}$ is the magnetic moment of the specimen in an applied magnetic field.

The average spacing between nearest neighboring crystals meticulously arranged on the Indium foil was about 0.25 mm. A numeral calculation using expression (3) reveals that the largest local external field in a crystal close to the center of the specimen was less than 1% of the applied field (in a low field) and never exceeds 4 Oe as the superconducting magnetization reached its largest value. Comparison of the applied field and the remnant magnetic field in the superconducting solenoid indicates that the local

external field seen by each crystal due to other crystals can be neglected. We note that this approach is not valid for a polycrystalline specimen due to a strong induction between touching crystals. Consistent with this argument, magneto-optical imaging (MOI) technique has confirmed that magnetic field distribution in a superconducting polycrystalline sample is more complex than that in a single crystal [6].

3. Results and discussion

Contactless measurements of the critical current density rely on measuring the magnetic moment of a superconductor in increasing and decreasing magnetic fields. Fig. 1 shows representative hysteresis loops for the Bi-2223 single crystals at $T = 5$ K and 34 K, respectively. They show an exponential decay of the width in the hysteresis loop, $\Delta \boldsymbol{M}$, with increasing the applied magnetic field. This exponential decrease is typical when the magnetic field is parallel to the *c*-axis of the crystal lattice. It is indicative of the strong field dependence of J_c in a material with a very weak pinning potential [4].

A conventional approach to determine the critical current density, J_c, from the width of magnetic hysteresis loop, $\Delta \boldsymbol{m}$, is Bean formula (in mks units):

$$J_c = \beta \frac{\Delta m}{a} \tag{4}$$

where β is geometry dependence factor, i.e. $\beta = 1$ for a slab of thickness $2a$ or $\beta = 3/2$ for a long cylinder of radius a and the same for a long specimen with square cross-section $2a \times 2a$ [1,7–9] Unfortunately, almost all single crystals of HTS materials are in a form of plates with the *c*-axis corresponding to the shortest direction. The bar-shaped specimen still has high symmetry, but, for the field aligned parallel to the *c*-axis, the critical state is much different from that of a slab or a long cylinder because of large demagnetization effects. A quantitative analysis, considering the demagnetization effects, has been developed by Brandt and Indenbom [10]:

$$\mathbf{M}_{\uparrow\downarrow}(\mathbf{H}_0) = \pm J_c(2d)a^2\left[\tanh\frac{\mathbf{H}_0}{\mathbf{H}_c} - 2\tanh\frac{\mathbf{H}_a \mp \mathbf{H}_0}{2\mathbf{H}_c}\right] \tag{5}$$

where $\boldsymbol{M}$ is the magnetic moment per unit length of a strip, in a perpendicular magnetic field $\boldsymbol{H}_a$; $\boldsymbol{H}_0$ is the maximum value of $\boldsymbol{H}_a$; a is the half-width of a specimen with thickness of $2d$; and $\boldsymbol{H}_c$ is a field related to J_c by $\boldsymbol{H}_c = J_c(2d)/\pi$. A detailed analysis for the field dependence of J_c in Bi-2223 single crystals will be discussed in a subsequent paper. Here, we emphasize that for applied field maximums, $\boldsymbol{H}_0 \gg \boldsymbol{H}_c$, the remnant magnetic moment per unit length at $\boldsymbol{H}_a = 0$, reducing Eq. (5), is

$$\mathbf{M}_{\mathrm{rem}}(\mathbf{H}_0) = J_c(2d)a^2 \tag{6}$$

and expression (4) is invariant on the a/d ratio. Using $\beta = 3/2$ in formula (4), the critical current density of Bi-2223 single crystals at zero applied field are shown in Fig. 2 as a function of temperature.

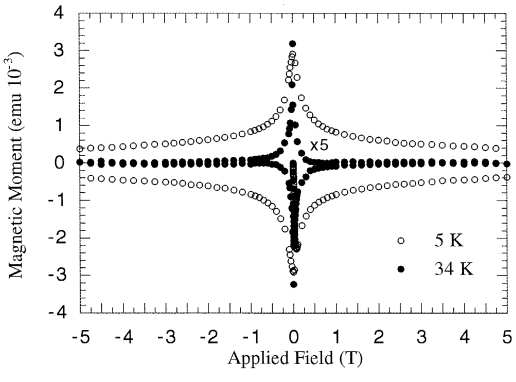

Fig. 1. Representative hysteresis loops of the Bi-2223 single crystals at $T = 5$ and 34 K, respectively.

Contactless AC methods for determining J_c values consider the flux profiles inside a specimen. Fig. 3 shows the temperature dependence of the real, $\boldsymbol{M}'$, and imaginary, $\boldsymbol{M}''$, parts of the AC magnetization for our specimen in various AC fields. No detectable contribution to the diamagnetic signal from the Bi-2212 phase was detected. The steps in $\boldsymbol{M}'(T)$ and the peaks in $\boldsymbol{M}''(T)$ shift to lower temperature as the amplitude of AC field, h_0, is raised from 0.5 Oe to 14.5 Oe, consistent with the increase in J_c at lower temperatures. A commonly used AC susceptibility

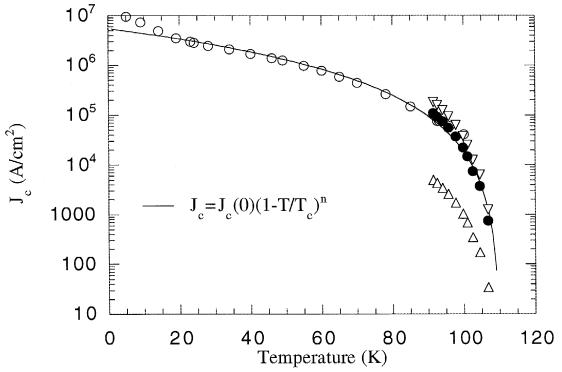

Fig. 2. Temperature dependence of critical current density of B-2223 single crystals at zero applied field. The AC data was extracted from imaginary part of magnetization as a function of temperature at varied AC field by using different formulas (Δ, ∇ and ● for using formulas (7)–(9), respectively).

technique to measure the critical current density consider the temperature, T_p, at which the maximum loss occurs, i.e. the peak in $\boldsymbol{M}''$. For a bulk specimen, $J_c(T_p)$ has the general form of:

$$J_c(T_p) \approx \alpha \frac{h_0}{a} \tag{7}$$

where $\alpha \sim 1$ is a geometry-dependent factor and a is the half-width of a slab or the radius of a long cylinder. A series of recently published papers based on numerical models and experimental results revealed that expression (7) extracted from the simple Bean model did not apply to disk specimens with AC fields applied in the axial direction where geometrical demagnetization effects are crucial [11–18]. In the case of our Bi-2223 single crystals, using relationship (7) may lead to unreasonably small values of J_c.

Using a modified Bean model, a similar relation for J_c in a thin film geometry, with an AC perpendicular magnetic field, was developed [13,15]:

$$J_c(T_p) \approx \alpha \frac{h_0}{2d} \tag{8}$$

where $2d$ is the thickness of the film. Although AC susceptibility of Y-123 and Hg-1212 thin films as a function of AC field showed an excellent agreement with the model, for a thick disk, relationship (8) may need to be modified. The J_c values extracted from both relationships (7) and (8) using our AC magnetization data have been presented in Fig. 2. For a bar with rectangular cross-sections $2a \times 2d$, Forkl [19] has determined an expression for the perpendicular penetration fields:

$$\mathbf{H}_p = J_c \frac{d}{\pi}\left[\frac{2a}{d}\arctan\frac{d}{a} + \ln\left(1+\frac{a^2}{d^2}\right)\right] \tag{9}$$

Substituting $a = 36.5$ μm, $d = 0.5$ μm and AC penetration field data shown in Fig. 3 in relation (9), we have presented the temperature dependence of critical current density of Bi-2223 single crystals in Fig. 2. Good agreement between the DC and AC analysis is observed.

The temperature dependence of critical current density of HTS materials commonly obeys an empirical scaling relation in a wide temperature range:

$$J_c = J_c(0)\left(1-\frac{T}{T_c}\right)^n \tag{10}$$

where $J_c(0)$ is the critical current density at $T = 0$ K. Using $T_c = 110$ K and the experimental data extracted from DC and AC magnetization by using formulas (4) and (9), respectively, a fitting curve to

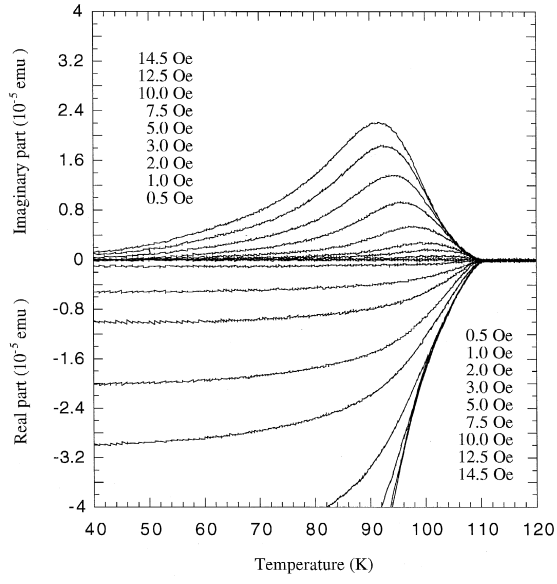

Fig. 3. Temperature dependence of the real part, $\boldsymbol{M}'$, and imaginary part, $\boldsymbol{M}''$, of the magnetization of Bi-2223 single crystals in various AC fields at a frequency $f = 83$ Hz.

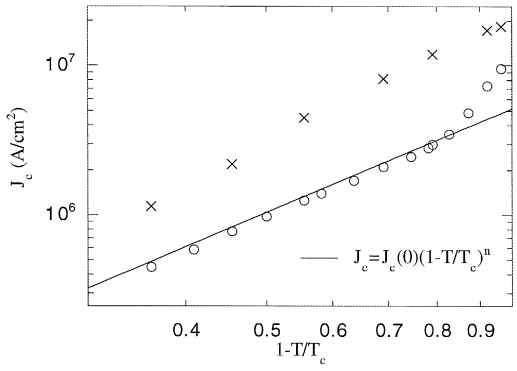

Fig. 4. Comparison of $J_c(T)$ between pristine (○) and irradiated (×) B-2223 single crystals at zero applied field.

the relation (10) gives $n = 2.37$ and $J_c(0) = 5.4 \times 10^6$ (A/cm^2).

A significant difference between the experimental J_c of pristine crystals and the fitting curve at $T < 20$ K is shown in Fig. 4. An upturn of J_c at low temperature implies stronger flux pinning. The pinning in this temperature range is consistent with estimates of the temperature range above which an ordered vortex solid becomes metastable [20,21]. A steep decline of J_c in zero applied field, with increasing temperature, can be explained by a weak pinning potential in the layered BSCCO system [4]. In order to examine the importance of introducing a strong pinning potential to enhance critical current density in this system, J_c values of irradiated Bi-2223 single crystals with 0.8 GeV protons at fluence of 7.0×10^{16} protons/cm^2 are shown in Fig. 4. Along with large enhancements of J_c, the deep decline of J_c at $T \sim 20$ K in the pristine crystals disappears, implying that the magnetic flux is effectively pinned by the columnar defects created by the proton tracks. Details of this investigation will be presented in subsequent papers.

4. Conclusion

The temperature dependence of the critical current density of Bi-2223 single crystals in zero applied field has been measured by contactless method for the first time. Modified Bean models were used to show that the J_c values extracted from DC remnant magnetic moment and AC susceptibility were consistent and obey the same empirical scaling relation for $T > 20$ K.

Acknowledgements

The authors gratefully acknowledge fruitful discussions with J.O. Willis and M.P. Maley of Los Alamos National Laboratory.

References

[1] M.E. McHenry, R.A. Sutton, Prog. Mater. Sci 38 (1994) 159.
[2] M.R. Cimberle, C. Ferdeghini, G. Grasso, C. Rizzuto, A.S. Siri, R. Flukiger, F. Marti, Supercond. Sci. Technol. 11 (1998) 837.
[3] S.-Y. Chu, M.E. McHenry, J. Mater. Res. 13 (1998) 589.
[4] S.-Y. Chu, M.E. McHenry, IEEE Trans. Appl. Supercond. 7 (1997) 1150.
[5] S.-Y. Chu, M.E. McHenry, Electrochem. Soc. Proc. 97-2 (1997) 9.
[6] J. Albrecht, Ch. Jooss, R. Warthmann, A. Forkl, H. Kronmuller, Phys. Rev. [Sect.] B 57 (1998) 10332.
[7] C.P. Bean, Phys. Rev. Lett. 8 (1962) 250.
[8] C.P. Bean, Rev. Mod. Phys. 36 (1964) 31.
[9] D.-X. Chen, R.B. Goldfarb, J. Appl. Phys. 66 (1989) 2489.
[10] E.H. Brandt, M. Indenbom, Phys. Rev. [Sect.] B 48 (1993) 12893.
[11] L.W. Conner, A.P. Malozemoff, Phys. Rev. [Sect.] B 43 (1991) 402.
[12] M. Daumling, D.C. Larbalestier, Phys. Rev. [Sect.] B 40 (1989) 9350.
[13] M. Wurlitzer, M. Lorenz, K. Zimmer, P. Esquinazi, Phys. Rev. [Sect.] B 55 (1997) 11816.
[14] J. Albrecht, Ch. Jooss, R. Warthmann, A. Forkl, H. Kronmuller, Phys. Rev. [Sect.] B 57 (1998) 10332.
[15] B.J. Jonsson, K.V. Rao, S.H. Yun, U.O. Karlsson, Phys. Rev. [Sect.] B 58 (1998) 5862.
[16] E.H. Brandt, Phys. Rev. [Sect.] B 58 (1998) 6506.
[17] E.H. Brandt, Phys. Rev. [Sect.] B 58 (1998) 6523.
[18] E.H. Brandt, Phys. Rev. [Sect.] B 54 (1996) 4246.
[19] A. Forkl, Phys. Scr., T 49 (1993) 148.
[20] M.F. Goffman, J.A. Herbsommer, F. de la Cruz, T.W. Li, P.H. Kes, Phys. Rev. [Sect.] B 57 (1998) 3663.
[21] M. Tinkham, Introduction to Superconductivity, Second edn., McGraw-Hill, NY, 1995.